ARL-TR-10324 ● APR 2026

Strategies for Postprocessing Non-Natural Modifications of Commercially Produced Magnetosomes

by Alexander Winton, Mark A. Allen, and Matthew Coppock

NOTICES

Disclaimers

The findings in this report are not to be construed as an official Department of the Army position unless so designated by other authorized documents.

Citation of manufacturer's or trade names does not constitute an official endorsement or approval of the use thereof.

Destroy this report when it is no longer needed. Do not return it to the originator.

ARL-TR-10324 ● APR 2026

Strategies for Postprocessing Non-Natural Modifications of Commercially Produced Magnetosomes

Alexander Winton, Mark A. Allen, and Matthew Coppock
DEVCOM Army Research Laboratory

REPORT DOCUMENTATION PAGE

1. REPORT DATE	2. REPORT TYPE	3. DATES COVERED	
April 2026	Technical Report	10/1/2023	9/30/2025

4. TITLE AND SUBTITLE
Strategies for Postprocessing Non-Natural Modifications of Commercially Produced Magnetosomes

5a. CONTRACT NUMBER	5b. GRANT NUMBER	5c. PROGRAM ELEMENT NUMBER
5d. PROJECT NUMBER	**5e. TASK NUMBER**	**5f. WORK UNIT NUMBER**

6. AUTHOR(S)
Alexander Winton, Mark A. Allen, and Matthew Coppock

7. PERFORMING ORGANIZATION NAME(S) AND ADDRESS(ES)	8. PERFORMING ORGANIZATION REPORT NUMBER
DEVCOM Army Research Laboratory ATTN: FCDD-RLA-HB Adelphi, MD 20783	ARL-TR-10324

9. SPONSORING/MONITORING AGENCY NAME(S) AND ADDRESS(ES)	10. SPONSOR/MONITOR'S ACRONYM(S)	11. SPONSOR/MONITOR'S REPORT NUMBER(S)

12. DISTRIBUTION/AVAILABILITY STATEMENT
DISTRIBUTION STATEMENT A. Approved for public release: distribution unlimited.

13. SUPPLEMENTARY NOTES

14. ABSTRACT
Magnetosomes are nanoscale magnetic particles encased in a phospholipid bilayer synthesized in magnetotactic bacteria. In this work, magnetosomes were characterized and chemically modified to explore their potential for bio-integration and material science applications. Fourier-transform infrared spectroscopy confirmed the presence of a phospholipid membrane surrounding the iron-oxide core of magnetosomes, differentiating them from commercially sourced magnetite. Initial attempts at aqueous dispersion proved challenging, with solvent viscosity positively correlating to suspension stability. Subsequent chemical modifications—utilizing fluorescein isothiocyanate, carbodiimide chemistry, and cholesterol anchoring—demonstrated successful surface functionalization. Biotinylation and cellulose binding peptide modification were also achieved, leading to the creation of magnetically responsive cotton textiles with approximately 5.5% (w/w) magnetite loading. These results provide a foundation for future genetic engineering and chemical modification strategies aimed at enhancing magnetosome functionality and biocompatibility.

15. SUBJECT TERMS
magnetosome, membrane modification, magnet, textile modification, Biological and Biotechnology Sciences

16. SECURITY CLASSIFICATION OF:			17. LIMITATION OF ABSTRACT	18. NUMBER OF PAGES
a. REPORT	b. ABSTRACT	C. THIS PAGE		
UNCLASSIFIED	UNCLASSIFIED	UNCLASSIFIED	UU	26

19a. NAME OF RESPONSIBLE PERSON	19b. PHONE NUMBER *(Include area code)*
Alexander Winton	(520) 691-5016

STANDARD FORM 298 (REV. 5/2020)
Prescribed by ANSI Std. Z39.18

Contents

List of Figures iv

List of Tables iv

1. Introduction 1

2. Materials and Methods 2

2.1 Fourier-Transform Infrared Spectroscopy (FTIR) 2

2.2 Transmission Electron Microscopy (TEM) 2

2.3 Magnetosome Modifications 2

2.3.1 Isothiocyanate Coupling 2

2.3.2 Carbodiimide Coupling 2

2.3.3 Cholesterol Membrane Anchoring 3

2.3.4 Biotin Quantitation 3

2.3.5 Fluorescein Assessment 3

2.4 Particle Dispersibility 3

2.5 Sodium Dodecyl Sulfate–Polyacrylamide Gel Electrophoresis (SDS-PAGE) 4

2.6 Cotton Textile Modification 4

2.7 Magnetic Measurements 4

3. Results and Discussions 4

3.1 Magnetosome Characterization 4

3.2 Chemical Modifications of Magnetosomes 8

3.3 Cellulose Modification 13

4. Conclusion 16

5. References 17

List of Symbols, Abbreviations, and Acronyms 19

Distribution List 20

List of Figures

Figure 1. A) FTIR spectra of different magnetite and phospholipid control samples. B) DSPC structure, a phospholipid found in cell membranes. 5

Figure 2. FTIR spectra of magnetite and magnetosome samples..... 6

Figure 3. TEM images of purified magnetosomes. 6

Figure 4. Magnetosome suspension stability in various solvents. 7

Figure 5. FTIR spectra of magnetosomes following exposure to different solvents. 8

Figure 6. A) Graphic cartoon of a magnetosome. B) Graphic cartoon of a magnetosome modified chemically with FITC. C) Graphic cartoon of a magnetosome modified using a cholesterol anchoring strategy. 9

Figure 7. FITC covalent linking reaction equation. 9

Figure 8. Assessment of FITC fluorescent intensity of modified magnetosomes exposed to different solvents. 10

Figure 9. A) Structure of FITC–PEGn–cholesterol. B) Structure of biotin–PEGn–cholesterol. 11

Figure 10. Fluorescence intensities observed for various magnetosome modification strategies. 11

Figure 11. Fluorescence intensity of wash supernatants following magnetosome chemical modification..... 12

Figure 12. Biotin quantitation assay of magnetosomes modified by various methods. 12

Figure 13. SDS-PAGE analyses of magnetosome samples. 13

Figure 14. A) Cotton textile samples after experimental treatment and washing. B) Magnetic response of modified cotton samples..... 14

Figure 15. A) Cartoon image depicting multiarm PEG modification of magnetosome membrane. B) Cartoon depicting CBD peptide modification of multiarm PEG-modified magnetosome membrane... 14

Figure 16. Magnetosome modification by multiarm PEG + CBD peptide..... 15

Figure 17. A) Thermogravimetric analysis of MgS modified cotton textile. B) Vibrational scanning magnetometry of MgS modified cotton textile. 15

List of Tables

Table 1. Characteristics of solvents assessed for magnetosome suspension. 7

1. Introduction

Magnetosomes are intracellular, membrane-bound nanocrystals of iron oxides produced by a diverse group of bacteria known as magnetotactic bacteria (MTB). These bacteria, ubiquitously found in aquatic sediments, align themselves with the Earth's magnetic field lines, facilitating navigation toward optimal environments. MTB actively synthesize magnetosomes, a process initiated by membrane invaginations where iron uptake and oxidation occur. Specialized proteins orchestrate the formation of highly ordered crystal structures, preventing iron precipitation as amorphous oxides.

Magnetosome composition typically consists of magnetite (Fe_3O_4) or greigite (Fe_3S_4), although most research effort is directed toward magnetite.[1,2] Minerals are encased within a lipid bilayer membrane composed of phospholipids and proteins. This bilayer, crucial for stability and preventing oxidation, is structurally similar to eukaryotic cell membranes. Magnetosomes are generally 20–120 nm in diameter, exhibiting a remarkably uniform size and shape—often resembling polyhedra or ellipsoids. This uniformity contributes to their exceptional magnetic properties.

Due to their crystalline structure and single-domain size, magnetosomes are prepared at a size very close to the superparamagnetic limit, which means that depending on the size of the particle, they can have superparamagnetic behavior (particles <25 nm) or they can behave like room temperature ferromagnets (particles >25 nm).[3] They respond rapidly to external magnetic fields, a key characteristic exploited in various applications.

The potential for both genetic and surface modifications expand magnetosome utility. Genetic engineering can alter the type of iron oxide produced, control particle size and shape, or introduce targeting ligands. Surface modifications, as demonstrated in recent research, involve conjugating antibodies, peptides, or polymers to the membrane, enhancing biocompatibility and enabling targeted delivery.

Applications are diverse, ranging from biomedical imaging and targeted drug delivery to environmental remediation (removing pollutants) and biosensors. Their biocompatibility makes them attractive for hyperthermia cancer therapy, while their magnetic properties are leveraged in magnetic resonance imaging contrast agents. Further development promises magnetosomes as tools for manipulating cells, creating novel biomaterials, and advancing nanotechnology.

2. Materials and Methods

2.1 Fourier-Transform Infrared Spectroscopy (FTIR)

Bruker Alpha Platinum attenuated total reflectance (ATR) FTIR was used to perform 24 scans, at 4-cm^{-1} resolution, 4000–400 cm^{-1}. Samples of magnetosomes and modified magnetosomes were analyzed as dry powders on an ATR crystal.

2.2 Transmission Electron Microscopy (TEM)

TEM was performed using a JEOL 2100F operating at 200 kV and imaging at several magnifications. Lacey Carbon TEM grids on 300-mesh copper (Ted Pella) were used.

2.3 Magnetosome Modifications

Sonication was performed with a FisherBrand Model 120 Sonic Dismembrator.

2.3.1 Isothiocyanate Coupling

Dried magnetosome particles (1 mg) were washed three times with 50-mM carbonate buffer pH 9. The particles were then resuspended in 1 mL of 50-mM carbonate buffer with 1 mg of fluorescein isothiocyanate (FITC) and sonicated using a sonic horn at 4 °C using a cycle of 1 s “on,” 1 s “off” for 30 min “on,” 30% amplitude. Then, the sample was washed three times with a phosphate-buffered saline (PBS) buffer pH 7.2 and resuspended to a final 1-mg/mL magnetosome concentration. Samples were washed three times with desired organic solvents and then washed twice with PBS before being resuspended to 1 mg/mL in PBS and assessed for fluorescent intensity.

2.3.2 Carbodiimide Coupling

Dried magnetosome particles (1 mg) were washed three times with 100-mM 2-morpholinoethanesulfonic acid (MES) buffer at pH 6. The particles were then resuspended in 1 mL of 10-mM MES pH 6. Next, 1-ethyl-3-[3-dimethylaminopropyl]carbodiimide (EDC) and N-hydroxysuccinimide (NHS) were added to the sample along with approximately 1–10 μM of the desired chemical agent to be coupled (fluorescein, biotin, peptide). The sample was then sonicated using a sonic horn at 4 °C using a cycle of 1 s on, 1 s off for 30 min on, 30% amplitude. Then, the sample was washed at least three times with PBS buffer pH 7.2 and resuspended to a final 1-mg/mL magnetosome concentration.

For samples in which a modifying ligand was previously modified by EDC/NHS (e.g., NHS-fluorescein, NHS-biotin), 1 mg of dried magnetosome particles were washed three times with 10-mM MES buffer pH 6. The particles were then resuspended in 1 mL of 10-mM MES pH 6, 1 mg of NHS activated labeling reagent was added, and the sample was sonicated using a sonic horn at 4 °C using a cycle of 1 s on, 1 s off for 30 min on, 30% amplitude. Then, the sample was washed at least three times with PBS buffer pH 7.2 and resuspended to a final 1-mg/mL magnetosome concentration.

2.3.3 Cholesterol Membrane Anchoring

Dried magnetosome particles (1 mg) were washed three times with 10-mM 4-(2-hydroxyethyl)-1-piperazineethanesulfonic acid (HEPES) buffer pH 7.2. The particles were then resuspended in 1 mL of 10-mM HEPES buffer pH 7.2 with 1–2 mg of cholesterol-PEG-fluorescein (2 kDa) or cholesterol-PEG-biotin (1 kDa) and sonicated using a sonic horn at 4 °C using a cycle of 1 s on, 1 s off for 30 min on, 30% amplitude. Next, the sample was washed three times with a tris-buffered saline (TBS) buffer pH 7.2 and resuspended to a final 1-mg/mL magnetosome concentration.

2.3.4 Biotin Quantitation

Biotinylated magnetosome samples (previously described) were then assessed for a qualitative presence of biotin to confirm successful labeling using a Thermo Scientific Pierce Fluorescence Biotin Quantitation Kit and its standard protocol. TBS buffer was used for the assay, and 100 µL of each 1-mg/mL magnetosome sample was used for each reading (readings were performed in duplicate).

2.3.5 Fluorescein Assessment

Fluorescently labeled magnetosome particles were excited at 492 nm and emission observed at 522 nm.

2.4 Particle Dispersibility

Dried magnetosome samples (1 mg) were resuspended in 1 mL of desired organic solvent and then sonicated using a sonic horn at 4 °C using a cycle of 1 s on, 1 s off for 30 min on, 30% amplitude. The sample was then vortexed for 5 s and the outer diameter at 600 nm was recorded every 2 min for 20 min.

2.5 Sodium Dodecyl Sulfate–Polyacrylamide Gel Electrophoresis (SDS-PAGE)

SDS-PAGE was run on a Mini-Protein TGX Precast Gel from Bio-Rad (4%–20% gradient) at 120 V for 45–60 min in 1×Tris/Glycine SDS Electrophoresis buffer (Bio-Rad). The gel was stained with Coomassie dye and destained using 10% acetic acid, 50% methanol, and 40% water. Magnetosomes samples were challenged with 1-mg streptavidin and washed three times with buffer prior to running on SDS-PAGE.

2.6 Cotton Textile Modification

Dried magnetosomes (8.7 mg) were resuspended with 87 mg of four Arm-NHS-PEG (1 kDa) in 8.7 mL of 10-mM MES pH 6 and then sonicated using a sonic horn at 4 °C using a cycle of 1 s on, 1 s off for 30 min on, 30% amplitude. The sample was then washed once with 10-mM MES pH 6 and resuspended in 8.7 mL of 10-mM MES pH 6 with 87 mg of cellulose binding domain (CBD) peptide (KSGSGCQVLNPWYSQTTPGWGQC, cyclized through disulfide linkage) and then sonicated using a sonic horn at 4 °C using a cycle of 1 s on, 1 s off for 30 min on, 30% amplitude. Next, the sample was washed twice with PBS + 0.1% Tween-20 and resuspended in 8.7 mL of PBS + 0.1% Tween-20. Then, 10 cotton circles (7-mm diameter) were added to the solution, and the sample was incubated at room temperature while shaking for 65 h followed by washing in PBS + 0.1% Tween-20 for 24 h.

2.7 Magnetic Measurements

Saturation magnetization and coercive forces were measured using cryogen-free VersaLab (Quantum Design) using vibrating sample magnetometry (sweeping ±3T) and performed at 100 and 300 K.

3. Results and Discussions

3.1 Magnetosome Characterization

Initial characterization of commercial magnetite, distearoylphosphatidylcholine (DSPC) templated magnetite, and DSPC was performed via FTIR to generate control spectra for subsequent magnetosome characterization. DSPC is a phospholipid that was selected because it mimics phospholipids that primarily compose cell and vesicle membranes of biological organisms. Magnetosomes are composed of an iron-oxide core and a bilayer membrane containing mostly

phospholipids and some proteins. Significant peaks observed for DSPC peaks at 2855 and 2920 cm^{-1} are from C-H group vibrations of methylene and methyl groups.[4] The peak at 2361 cm^{-1} may result from presence of CO_2 and is present in metal oxide, although intensity varies.[4] The peak at 1620 cm^{-1} arises from water molecules adsorbed to the inorganic surface (O-H bending).[5] The two peaks at 1405 and 1612 cm^{-1} result from stretching of carboxylate (COO) ions adsorbed to the inorganic surface and is present as a residual component of the magnetite synthesis.[6] Distinctly notable in the DSPC spectrum and somewhat visible in the DSPC-magnetite spectrum in a peak at 1060 cm^{-1} indicates the presence of a phospholipid on the in-house synthesized magnetite and corresponds to the P = O stretch arising from the phosphodiester moiety of the phospholipid.[7,8] This peak is absent from commercially pure magnetite. The band at 550 cm^{-1} may be attributed to Fe^{2+} – O^{2-} vibration from the iron-oxide particles.[5]

In the second FTIR spectra, a significantly observable peak at 1060 cm^{-1} in the magnetosome spectrum is observed, indicating the presence of phospholipids. This peak, along with TEM imaging, indicates the presence of a phospholipid bilayer in processed magnetosomes from Superbrewed Food, Inc. Peaks arising in the 3000–3500 cm^{-1} portions of the spectra correspond to O-H and N-H stretching. The broad stretch observed in this region of the magnetosome spectrum likely includes these O-H and N-H stretches associated with the biological components, such as proteins and phospholipids, but adsorbed water is likely the dominating contributor to this peak.[9] Peaks at 2351 and 2331 cm^{-1} are observed in the magnetosome sample and are not arising from a biological molecule. Since the peaks are present in magnesium sulfide (MgS), it is not likely arising as a distinct result of inorganic synthesis (as may have initially been inferred by the peak at 2361 cm^{-1} in Figure 1).

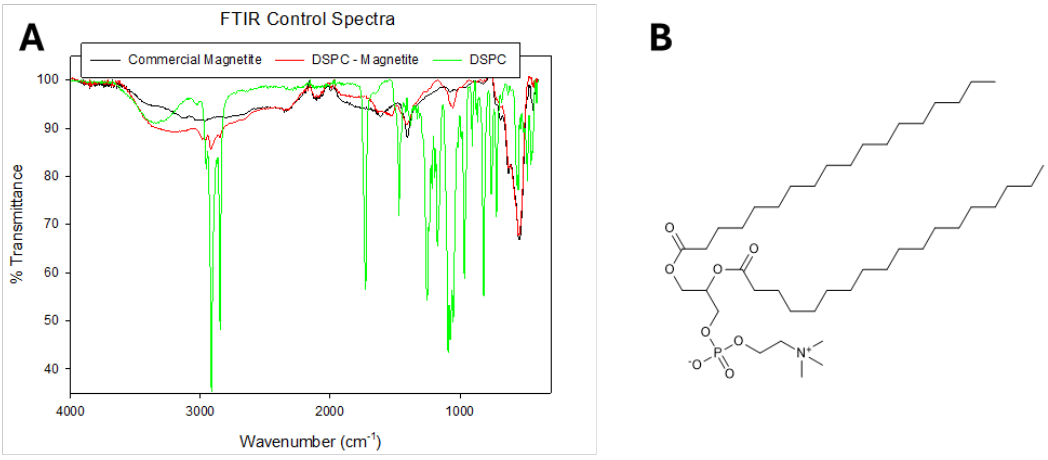

Figure 1. A) FTIR spectra of different magnetite and phospholipid control samples. B) DSPC structure, a phospholipid found in cell membranes.

They most effectively align with CO_2 spectrum and are likely arising from the dissolved and adsorbed gas.[10] The broad peak from 1730 to 1960 cm^{-1} is primarily present in the magnetosome sample. This is therefore likely arising from the uniqueness of the magnetosome membrane and proteins. It corresponds to carbonyl stretches—specifically, those of the phospholipid membrane—but is broadened due to interactions with water.[11] The presence of adsorbed water in the MgS sample is further confirmed by the broad peak from 3000 to 3500 cm^{-1}. The peak at 1643 cm^{-1} in the magnetosome spectrum corresponds to a C = O stretch in proteins and is termed the amide I band.[12] Participation in hydrogen bonding with water results in peak shifting to lower frequencies.[12] The magnetosome peak at 1536 cm^{-1} also correlates significantly to protein in the sample with the region from 1500 to 1600 cm^{-1} and known as the amide II band region; it comprises mainly N-H bending vibrations associated with peptide bonds.[12] TEM imaging also depicts small gaps and limited aggregation of magnetosome particles, which in conjunction with the observed FTIR spectra are indicative of the presence of phospholipids and proteins composing a membrane for the inorganic core. See Figures 2 and 3.

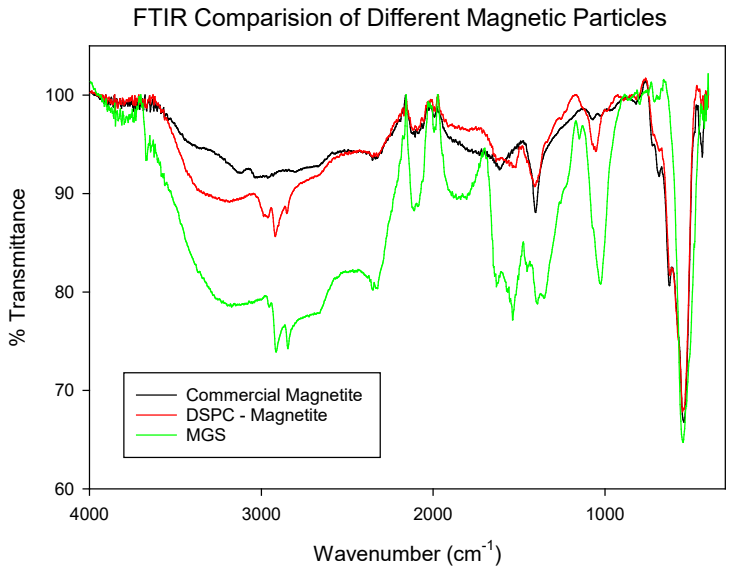

Figure 2. FTIR spectra of magnetite and magnetosome samples.

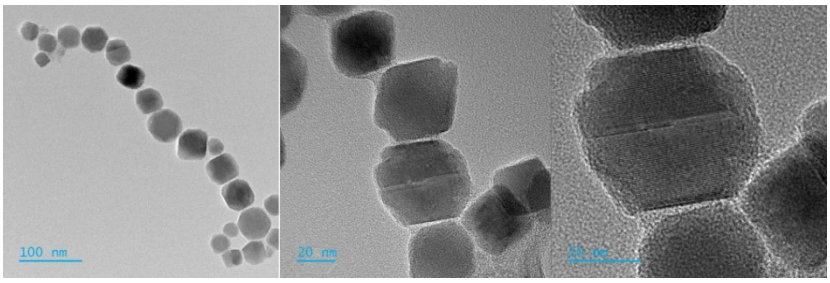

Figure 3. TEM images of purified magnetosomes.

Processed magnetosomes exhibited poor dispersibility in aqueous solution and settled out of solution rapidly, thereby prohibiting particle characterization by dynamic light scattering (DLS). Initial experiments with dispersing agents, such as nonionic detergent and glycerol, failed to effectively suspend magnetosome particles; therefore, alternative solvents were assessed for particle suspensions. Dry magnetosome samples were resuspended in organic solvents using sonication and the suspension stability was assessed optically based on turbidity measurements at 600 nm over a 20-min time course. In Figure 4, it was observed that tetrahydrofuran and methanol proved least effective for suspending magnetosomes, while 1-methyl-2-pyrrolidinone and 2-propanol were most effective. Assessment of solvent characteristics (Table 1) depicted a positive correlation between solvent viscosity and magnetosome suspension stability.[13] Therefore, more viscous organic solvents may provide a means for prolonging processed magnetosome suspensions in solutions.

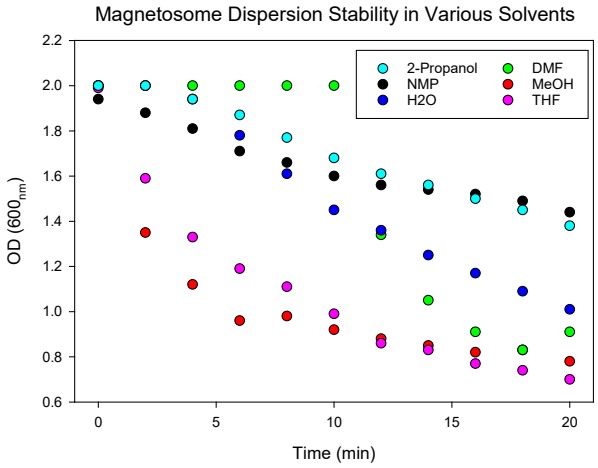

Figure 4. Magnetosome suspension stability in various solvents.

Table 1. Characteristics of solvents assessed for magnetosome suspension.

Solvent	Density	Viscosity (cp, 20 °C)	Refractive index (20 °C)
2-propanol	0.785	2.86 (15)	1.377
1-methyl-2-pyrrolidinone	1.028	1.67 (25)	1.47
Water	1	1	1.333
N, N-dimethylformamide	0.944	0.92	1.43
Methanol	0.791	0.55	1.329
Tetrahydrofuran	0.889	0.55	1.407

FTIR spectra of magnetosomes exposed to various organic solvents was performed to assess the impact on biological membrane components (Figure 5). Lyophilized samples of magnetosomes that had been exposed to various organic solvents were assessed via FTIR. Peak degradation and loss of definition were observed for peaks in the C-H region (2855 and 2920 cm^{-1}), the P = O stretch at 1060 cm^{-1}, and the amide II region peak at 1536 cm^{-1}. This was indicative of negative solvent impacts on the biological membrane of the magnetosomes.

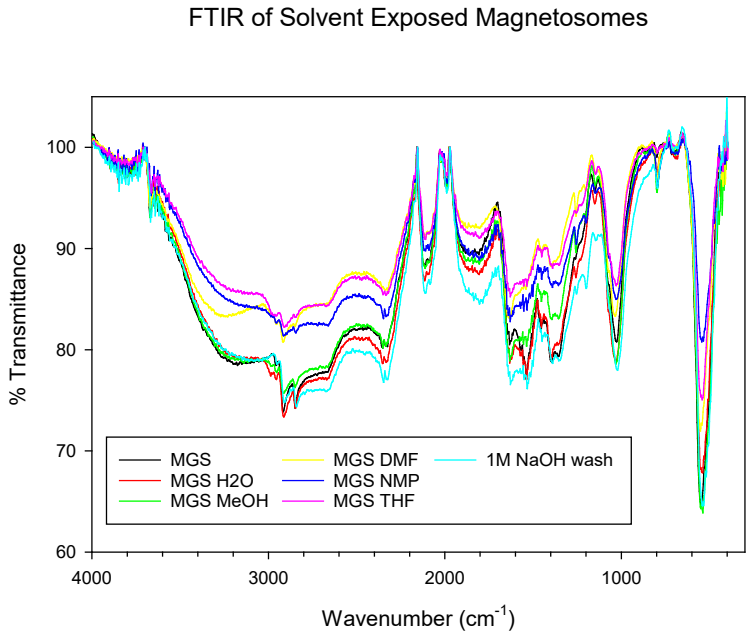

Figure 5. FTIR spectra of magnetosomes following exposure to different solvents.

3.2 Chemical Modifications of Magnetosomes

To develop a foundational understanding for future genetic engineering, chemical modifications of magnetosome membrane proteins and the magnetosome membrane were conducted (Figure 6). Covalent and noncovalent methodologies were employed to demonstrate successful chemical modifications with preliminary qualitative and quantitative assessment goals aimed at informing the value of genetic engineering.

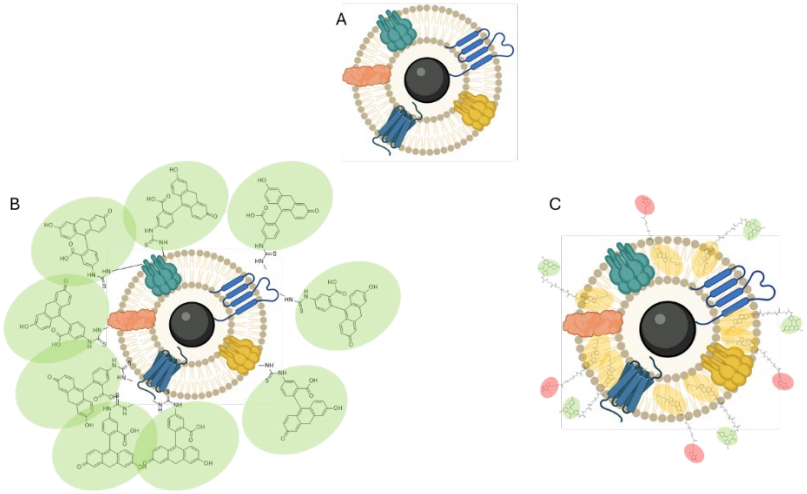

Figure 6. A) Graphic cartoon of a magnetosome. B) Graphic cartoon of a magnetosome modified chemically with FITC. C) Graphic cartoon of a magnetosome modified using a cholesterol anchoring strategy.

Covalent fluorescent modification of magnetosomes was initially performed using isothiocyanate chemistry, where FITC was incubated with magnetosomes while sonicating in carbonate buffer (Figure 8). This resulted in an overflow fluorescent reading that is displayed as a 60,000 fluorescent intensity unit cutoff. Magnetosome control in buffer exhibited some background fluorescence. Magnetosomes that were labeled covalently with FITC and subsequently washed with organic solvents (DMF, DMSO, or EtOH) demonstrated a loss of fluorescent intensity likely resulting from damage/stripping to the biological membrane of the magnetosomes (Figure 7).

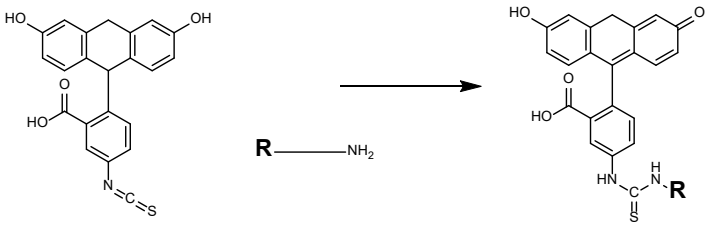

Figure 7. FITC covalent linking reaction equation.

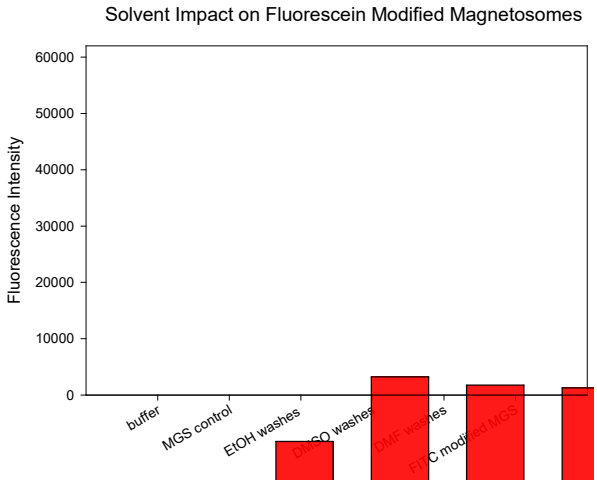

Figure 8. Assessment of FITC fluorescent intensity of modified magnetosomes exposed to different solvents.

Covalent fluorescence modification was also performed by carbodiimide chemistry, which utilizes 1-EDC and NHS to activate carboxylic acid moities (in this case the fluorescence molecule) for subsequent covalent coupling to amines found in the biomolecules composing the membrane and noncovalent membrane anchoring using a cholesterol (Figure 9). In the case of cholesterol-based anchoring, a cholesterol–polyethylene glycol–fluorescein was used. Comparisions between the two modification methods indicate a higher degree of fluorescence when performing the covalent modifications (Figure 10). Repeated washing of fluorescently modified samples was performed to ensure that residual, nonbound dye molecules were removed and that there was relative stability of the fluorescently labeled membrane. Figures for washing of cholesterol anchored and covalently bound fluorescein indicate that most nonbound dye is removed after two washes, where the wash supernatant was assessed for the presence of fluorescein (Figure 11). This indicates that the fluorescen observed by modified magnetosomes—after modification and washing—is relatively stable.

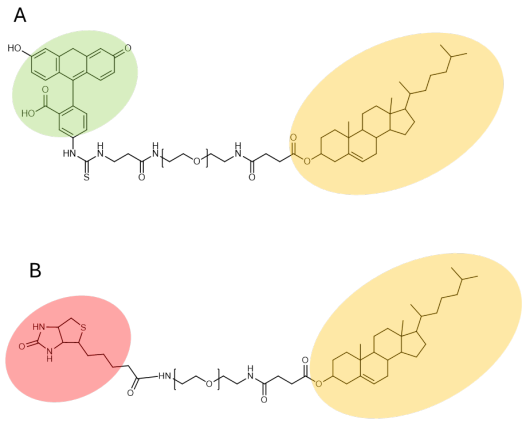

Figure 7. A) Structure of FITC–PEGn–cholesterol. B) Structure of biotin–PEGn–cholesterol.

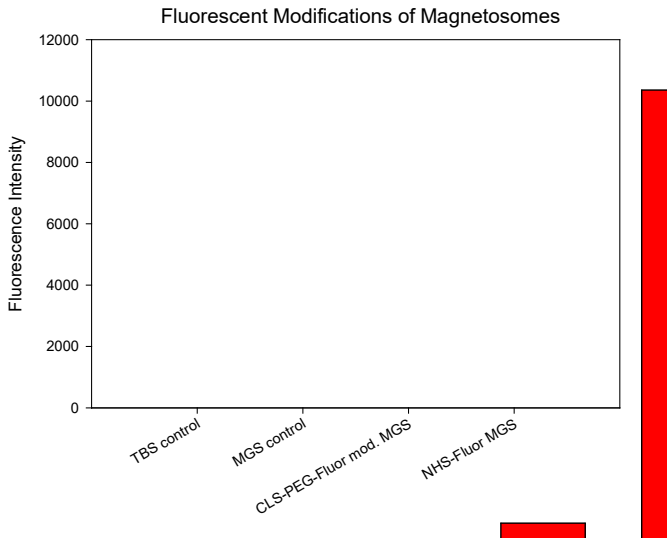

Figure 8. Fluorescence intensities observed for various magnetosome modification strategies.

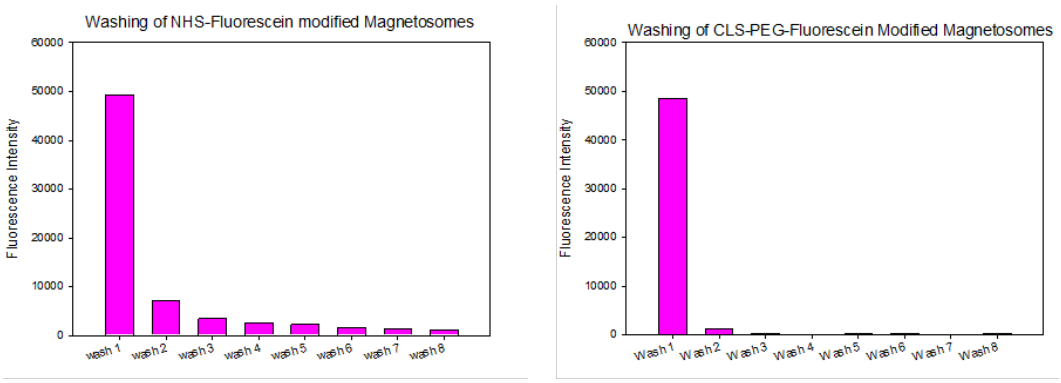

Figure 9. Fluorescence intensity of wash supernatants following magnetosome chemical modification.

Following successful fluorescence modifications, the potential for biotin modification (small molecule) was subsequently assessed. Biotin is a small molecule known to bind to the streptavidin protein with exceptional affinity. Assessment of this system would enable characterization of small-molecule modifications to magnetosome membranes, which would enable subsequent anchoring to potential material sets. Biotin modification of magnetosomes was carried out using either a cholesterol anchor or carbodiimide coupling chemistry. Qualitative assessment of biotinylation was performed using a biotin quantitation assay in which the presence of biotin displaces a modified 4'-hydroxyazobenzene-2-carboxylic acid (HABA), a fluorescent dye molecule initially bound to streptavidin. The resulting fluorescence measurements are directly proportional to the quantity of biotin present. Here, carbodiimide chemistry demonstrated superior quantity of modifications relative to using a cholesterol anchor (Figure 12).

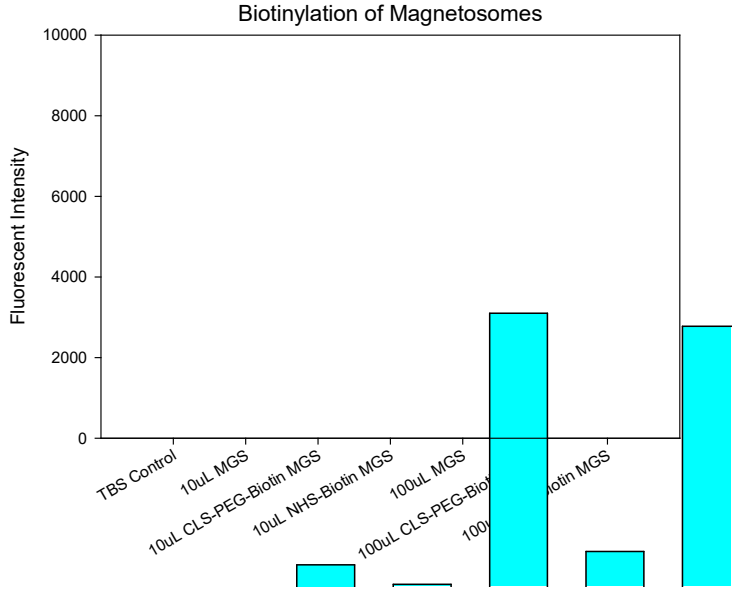

Figure 10. Biotin quantitation assay of magnetosomes modified by various methods.

Previous validations of magnetosome modifications relied on fluorescent measurements; therefore, another means of confirming successful magnetosome modifications was sought. The use of SDS-PAGE is commonly used for assessing proteins found in biological samples, and this methodology was subsequently used to assess magnetosome membrane protein content and probe sample for successful modification. Magnetosomes were biotinylated and incubated with streptavidin followed by an assessment on an SDS-PAGE gel. It was theorized that biotinylation of the magnetosome membrane would result in significant anchoring of streptavidin proteins, which may be visualized by the appearance of a band at about 55 kDa. In the gel image, it can be clearly depicted that large bands corresponding to streptavidin can be observed for both cholesterol anchoring and carbodiimide-based membrane biotinylation. Another notable observation is the significant lack of other proteins, with a majority of the observed protein bands appearing as 15 kDa or less (Figure 13). SDS-PAGE analyses performed on magnetosomes by other researchers indicated many proteins across a wide range of molecular weights.[14]

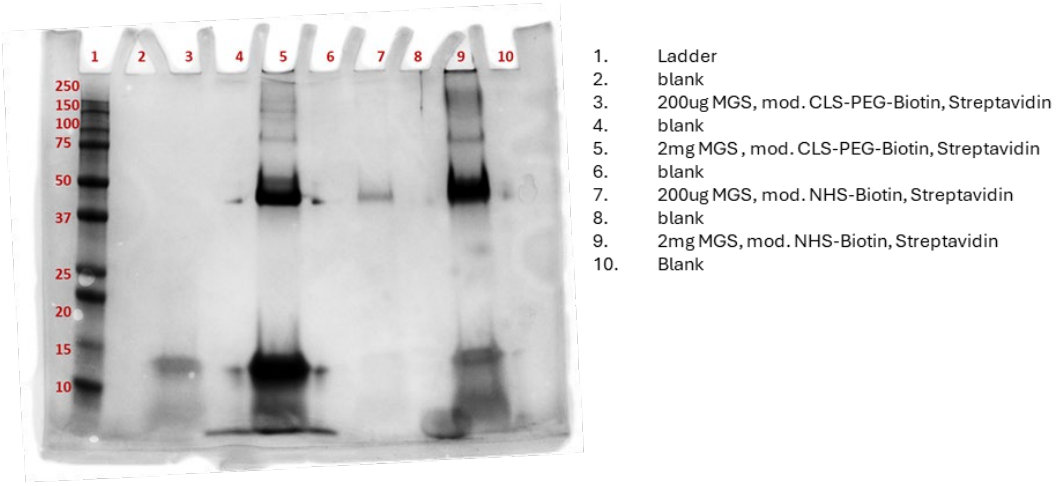

Figure 11. SDS-PAGE analyses of magnetosome samples.

3.3 Cellulose Modification

Initial modification of magnetosomes with a cellulose binding peptide (CBP) was carried out through carbodiimide chemistry utilized for fluorescent modification.[15,16] Following preparation, these modified magnetosomes were incubated with a cotton textile swatch (~1 × 1 cm). This resulted in a gray-to-black textile. However, upon washing, much of the color was lost, likely indicating poor magnetosome integration. When exposed to a magnet, this textile failed to exhibit magnetic affinity (Figure 14). Determination of effective peptide coupling presented challenges as the presence of protein fragments and phospholipids make it challenging to biochemical study of CBP linkage. Therefore, another method was

proposed for CBP modification of magnetosomes. This involved incubating magnetosomes with multiarm, n-hydroxy succinimide biotinyl(polyethyleneglycol) (PEG) followed by incubation with CBP (Figure 15). Following textile incubation and washing, this swatch retained a gray color and demonstrated attraction to a magnet. The incorporation of preactivated, multiarm PEG likely provided significantly more binding sites, as the NHS-PEG would theoretically interact with the primary amines of the phospholipid membrane, thereby providing more binding sites for the N-terminal amine of the CBP to covalently bind. The multiarm PEG modification was then performed again on cotton textile samples produced using a hole punch to control sample size. These circular samples also appeared to be successfully modified by MgS (Figure 16).

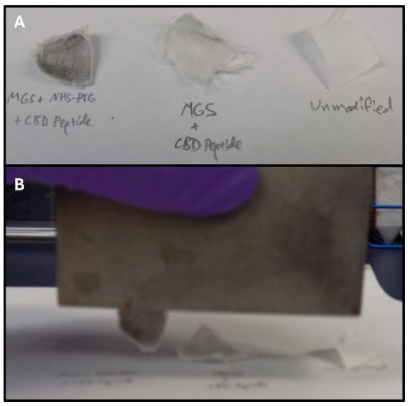

Figure 12. A) Cotton textile samples after experimental treatment and washing. B) Magnetic response of modified cotton samples.

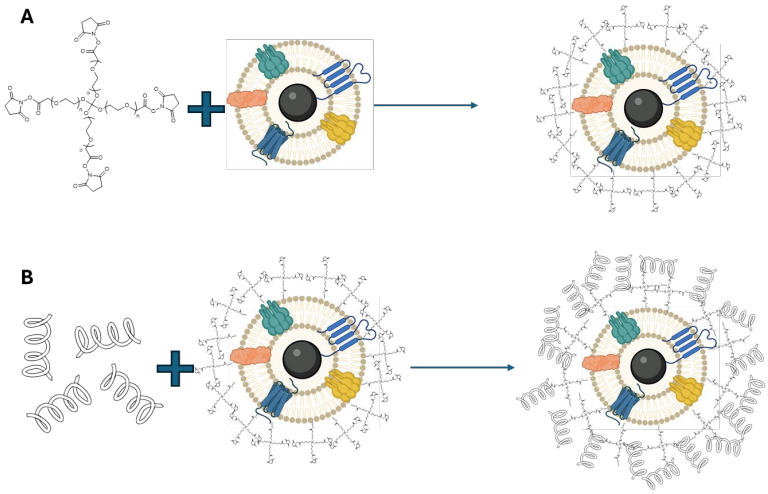

Figure 13. A) Cartoon image depicting multiarm PEG modification of magnetosome membrane. B) Cartoon depicting CBD peptide modification of multiarm PEG-modified magnetosome membrane.

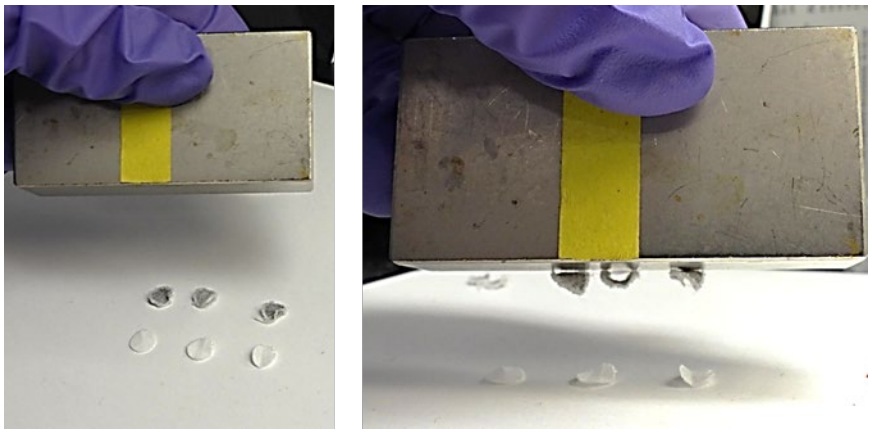

Figure 14. Magnetosome modification by multiarm PEG + CBD peptide.

Thermogravimetric analysis was next performed under a nitrogen atmosphere on MgS modified and unmodified textile samples to estimate the effective loading of magnetosomes (Figure 17). Both samples maintained a small amount of mass that was inorganic (likely, pyrolyzed carbon) after heating to 850 °C. A similar amount of each mass was analyzed via thermal analysis and indicated roughly 5.5% (w/w%) loading of magnetic particles into the cotton textile. Following thermal analysis, vibrating sample magnetometry was performed on MgS modified and unmodified samples to assess the magnetic properties. Cellulose alone exhibited a diamagnetic signal of –1.73 emu/g, the saturation magnetization of MgS modified cellulose was 9.09 emu/$g_{(magnetite)}$. Adding the negative contribution from cellulose alone would indicate an M_s of 10.82 emu/g based on total inorganic content. The magnetosome sample also showed a coercive field of 43 Oe, while the cellulose alone gave no hysteresis.

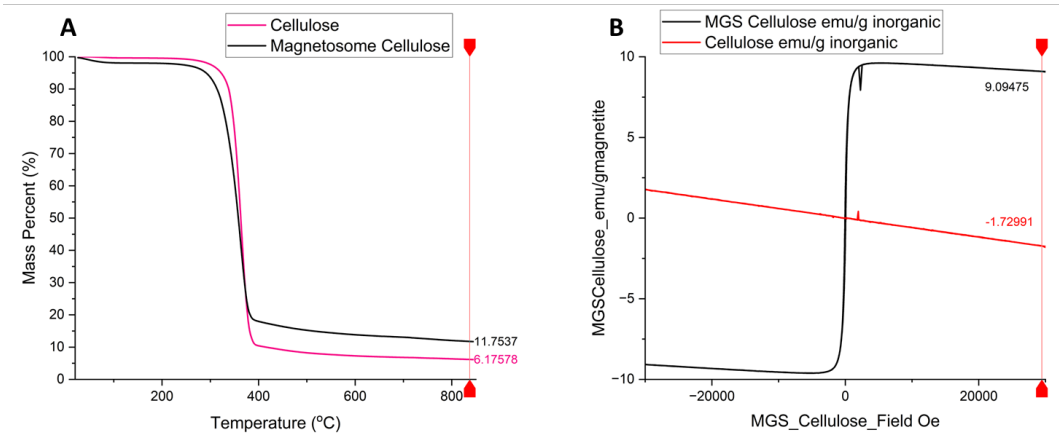

Figure 15. A) Thermogravimetric analysis of MgS modified cotton textile. B) Vibrational scanning magnetometry of MgS modified cotton textile.

4. Conclusion

This study successfully characterized and modified magnetosomes (i.e., nanoscale magnetic particles encased in a biological membrane). FTIR confirmed a phospholipid bilayer surrounding an iron-oxide core, distinguishing these from commercial magnetite. Dispersibility proved challenging, with viscous solvents like 1-methyl-2-pyrrolidinone offering improved suspension. Solvent exposure negatively impacted membrane integrity, as evidenced by FTIR signal loss. Chemical modifications using FITC, EDC/NHS, and cholesterol-PEG were achieved, with carbodiimide chemistry yielding superior fluorescent labeling. Processing methodology should be scrutinized to prevent membrane component degradation (as evidenced by protein breakdown observed in SDS-PAGE). Biotinylation and cellulose peptide modification demonstrated further potential for functionalization, culminating in magnetic cotton textiles with approximately 5.5% magnetite loading.

5. References

1. Faivre D et al. Intracellular magnetite biomineralization in bacteria proceeds by a distinct pathway involving membrane-bound ferritin and an iron(II) species. Angew Chem Int Ed. 2007;46(44):8495–8499.

2. Faivre D, Schuler D. Magnetotactic bacteria and magnetosomes. Chem Rev. 2008;108(11):4875–4898.

3. Alphandéry E et al. Difference between the magnetic properties of the magnetotactic bacteria and those of the extracted magnetosomes: influence of the distance between the chains of magnetosomes. J Phys Chem C. 2008;112(32):12304–12309.

4. Giri J et al. Preparation and characterization of phospholipid stabilized uniform sized magnetite nanoparticles. J Magn Magn Mater. 2005;293(1):62–68.

5. Silva C et al. Magnetic solid-phase microextraction for lead detection in aqueous samples using magnetite nanoparticles. J Braz Chem Soc. 2020;31(1):109–115.

6. Chen F et al. Synthesis and characterization of magnetite dodecahedron nanostructure by hydrothermal method. J Magn Magn Mater. 2008; 320(11):1775–1780.

7. Dluhy R, Wright N, Griffiths P. In situ measurement of the FT-IR spectra of phospholipid monolayers at the air water interface. Appl Spectrosc. 1988;42(1):138–141.

8. Derenne A, Vandersleyen O, Goormaghtigh E. Lipid quantification method using FTIR spectroscopy applied on cancer cell extracts. Biochim Biophys Acta-Mol Cell Biol Lipids. 2014;1841(8):1200–1209.

9. Kandori K, et al. Texture and formation mechanism of fibrous calcium hydroxyapatite particles prepared by decomposition of calcium-EDTA chelates. J Am Ceram Soc. 1997;80(5):1157–1164.

10. Köck E et al. In situ FT-IR spectroscopic study of CO_2 and CO adsorption on Y_2O_3, ZrO_2, and yttria-stabilized ZrO_2. J Phys Chem C. 2013;117(34):17666–17673.

11. Coates J. Interpretation of infrared spectra, a practical approach. Encyclopedia of Analytical Chemistry: Applications, Theory and Instrumentation. John Wiley & Sons, Ltd; 2006 Sep 15.

12. Haris P. Probing protein-protein interaction in biomembranes using Fourier transform infrared spectroscopy. Biochim Biophys Acta-Biomembr. 2013; 1828(10):2265–2271.

13. Sigma-Aldrich. Physical properties of solvents. 2025 Jan 29.

14. Grünberg K et al. A large gene cluster encoding several magnetosome proteins is conserved in different species of magnetotactic bacteria. App Environ Microbiol. 2001;67(10):4573–4582.

15. Linder M et al. Characterization of a double cellulose-binding domain – synergistic high affinity binding to crystalline cellulose. J Biol Chem. 1996;271(35):21268–21272.

16. van Zyl E, Coburn J. Functionalization of bacterial cellulose with the antimicrobial peptide KR-12 via chimerical cellulose-binding peptides. Int J Mol Sci. 2024;25(3).

List of Symbols, Abbreviations, and Acronyms

ATR	Attenuated Total Reflectance
CBD	Cellulose Binding Domain
CBP	Cellulose Binding Peptide
COO	Carboxylate
DLS	Dynamic Light Scattering
DMF	Dimethylformamide
DMSO	Dimethyl Sulfoxide
DSPC	Distearoylphosphatidylcholine
EDC	1-Ethyl-3-[3-Dimethylaminopropyl]Carbodiimide
EtOH	Ethanol
Fe_3O_4	Magnetite
Fe_3S_4	Greigite
FITC	Fluorescein Isothiocyanate
FTIR	Fourier-Transform Infrared Spectroscopy
HABA	4'-Hydroxyazobenzene-2-Carboxylic Acid
HEPES	4-(2-Hydroxyethyl)-1-Piperazineethanesulfonic Acid
MES	2-Morpholinoethanesulfonic Acid
MgS	Magnesium Sulfide
MTB	Magnetotactic Bacteria
NHS	N-Hydroxysuccinimide
PBS	Phosphate-Buffered Saline
PEG	Biotinyl(Polyethyleneglycol)
SDS-PAGE	Sodium Dodecyl Sulfate–Polyacrylamide Gel Electrophoresis
TBS	Tris-Buffered Saline
TEM	Transmission Electron Microscopy

1 (PDF)	DEFENSE TECHNICAL INFORMATION CTR DTIC OCA
1 (PDF)	DEVCOM ARL FCDD RLB CB TECH LIB